Thermotropic lanthanidomesogens

Claude Piguet,*[a] Jean-Claude G. Bünzli,*[b] Bertrand Donnio[c] and Daniel Guillon[c]

Received (in Cambridge, UK) 24th April 2006, Accepted 4th July 2006
First published as an Advance Article on the web 15th August 2006
DOI: 10.1039/b605737c

Due to their high and variable coordination numbers leading to poorly predictable three-dimensional coordination spheres, the trivalent lanthanide metal ions are challenging molecular objects for introduction into thermotropic liquid crystals. Conversely, their predictive electronic, optical and magnetic metal-centred properties make them particularly attractive for being incorporated into switchable macroscopic materials responding to external electric and magnetic stimuli. We briefly describe here some of the important concepts and strategies leading to the recent successful preparation of luminescent thermotropic lanthanide-containing mesophases, for which the generic term *lanthanidomesogens* is proposed.

1. Introduction

As judiciously asserted by Bruce in his seminal Dalton Perspective published in 1993, 'metal-containing liquid crystals are not simply obtained by adding long alkyl chains onto your favorite molecules—at least usually!' Some specific structural and electronic criteria, among which anisometry and polarizability, are of crucial importance for successfully designing metallomesogens (*i.e.* metal-containing liquid crystals).[1,2] However, there is a recurrent and cumbersome trend in metallomesogens for systematically providing counter-examples to any structural rules or guidelines, as soon as the latter tend to reach a general agreement within the community. Let us illustrate this statement with two examples. Firstly, the simple lanthanide alkanoates made up of ionic salts involving trivalent Ln^{III} cations (Ln = La, Ce. Pr and Nd) and lipophilic carboxylates (often referred to as lanthanide 'soaps'), readily produce lamellar (smectic) thermotropic liquid crystals,[3] while more sophisticated strategies and designs based on engineered amphipathic lanthanide complexes display poor, if any, thermotropic properties.[4,5] Secondly, the generally accepted rules for organic liquid crystals, which claim that nematic or lamellar (often smectic) organizations in mesophases require rod-like molecules, while columnar organization is produced

[a]*Department of Inorganic, Analytical and Applied Chemistry, University of Geneva, 30 quai Ernest Ansermet, CH-1211 Geneva 4, Switzerland. E-mail: Claude.Piguet@chiam.unige.ch*
[b]*École Polytechnique Fédérale de Lausanne (EPFL), Laboratory of Lanthanide Supramolecular Chemistry, BCH 1402, CH-1015 Lausanne, Switzerland. E-mail: Jean-Claude.Bunzli@epfl.ch*
[c]*Institut de Physique et Chimie des Matériaux de Strasbourg–IPCMS, Groupe des Matériaux Organiques, 23 rue du Loess, B.P. 43, F-67034 Strasbourg Cedex 2, France*

Claude Piguet

Claude Piguet earned a PhD degree in 1989 from the University of Geneva in the field of biomimetic copper-dioxygen complexes. After postdoctoral periods in the groups of professors J.-M. Lehn, A. F. Williams, and J.-C. G. Bünzli, he initiated research projects in lanthanide supramolecular chemistry. In 1995 he received the Werner Medal of the New Swiss Chemical Society and was appointed in 1999 as full professor of inorganic chemistry at the University of Geneva. He has coauthored more than 130 scientific articles in various fields of chemistry, which include the design of discrete multimetallic supramolecular edifices and the unravelling of the thermodynamic origin of their self-assembly processes, the programming of novel electronic functions depending on intermetallic communications, the molecular tuning of local dielectric constants, the preparation of lanthanide-containing metallomesogens and the development of paramagnetic NMR methods for addressing solution structures.

Jean-Claude Bünzli

Jean-Claude Bünzli is a physical-inorganic and analytical chemist by training and an active researcher in the field of co-ordination and supramolecular chemistry of the lanthanide ions. He earned a degree in chemical engineering in 1968 and a PhD in 1971 from the École Polytechnique Fédérale de Lausanne (EPFL). He spent two years at the University of British Columbia and one year at the Swiss Federal Institute of Technology in Zürich before being appointed at the University of Lausanne in 1974. Since 2001 he has been full professor of inorganic chemistry at EPFL. His research focuses mainly on the relationship between luminescent properties and structure of lanthanide-containing materials, on the use of lanthanide ions as luminescent probes and on the design of self-assembled building blocks for the synthesis of materials with predetermined photophysical and magnetic properties.

This journal is © The Royal Society of Chemistry 2006

by disk-like molecules are not always obeyed in metallomesogens.[2] This is especially true for the tentative incorporation of bulky three-dimensional metallic cores into thermotropic liquid crystalline phases.[6] Trivalent lanthanides, which adopt high coordination numbers (usually CN = 8–9), but display no ligand-field and no pronounced stereochemical preference,[7] are typical examples, in which serendipity has been one of the most successful strategy for designing novel metallomesogens.[4] However, recent attempts, which aim at combining thermodynamic, material and coordination concepts, have brought some rationalization in the preparation of lanthanide-containing metallomesogens, tentatively termed *lanthanidomesogens* in this contribution.[8–13] In this feature article, we focus on novel developments in lanthanidomesogens, which are indebted to two novel strategies, (i) the use of pro-mesogenic polycatenar ligands and (ii) the decoupling of rigid cores from the lanthanide coordination sphere, in addition to the original embedding of bulky Ln^{III} into protected internal cavities. Particular attention is dedicated to the exploitation of the metal-centred optical properties brought by the lanthanides in liquid crystalline phases. Since our specific contribution to the bottom-up design of lanthanidomesogens has been recently reviewed,[14] we focus here on a more general discussion, in which coordination, thermodynamic and structural aspects are successively addressed.

2. Some basic coordination background for designing thermally stable lanthanide complexes

As a result of the different degrees of stabilization experienced by the 4f, 5d and 6s orbitals occurring upon ionization of the neutral metal, the fifteen lanthanide elements (Ln = La–Lu, Z = 57–71) exist almost exclusively in their trivalent state ([Xe]4f^n, n = 0–14) in coordination complexes.[7] Moreover, the valence 4f^n shell is screened from external perturbation by outer filled 5s^2 and 5p^6 shells, which (i) mainly restricts metal–ligand bonds to electrostatic interactions, (ii) retains atomic optical and magnetic properties in coordination complexes and (iii) produces only negligible ligand-field stabilization energies. Points (i) and (iii), combined with the large electrostatic factors encountered for Ln^{3+} ($8.7 < z^2/R_{CN\,=\,9} < 10.5$) provide variable and large coordination numbers ($6 \leqslant CN \leqslant 12$), and no pronounced stereochemical preference for Ln^{III} in the final complexes. Their description as the 'chameleons' of coordination chemistry is thus not usurped, although standard solvates and complexes usually possess CN = 8 associated with square antiprismatic or dodecahedron geometries, or CN = 9 associated with tricapped trigonal prismatic or monocapped square antiprismatic geometries.[7] According to a thermodynamic point of view, the net complexation reaction of a Ln^{III} ion with a ligand L^{x-} can be partitioned into two successive reactions shown in equilibria (1) and (2) (Solv = solvent):

$$[Ln(Solv)_n]^{3+} + [L(Solv)_p]^{x-} \leftrightarrows [Ln(Solv)_m]^{3+} + [L(Solv)_q]^{x-} + (n - m + p - q)\ Solv \quad (1)$$

$$[Ln(Solv)_m]^{3+} + [L(Solv)_q]^{x-} \leftrightarrows [LnL(Solv)_{m+q}]^{(3-x)+} \quad (2)$$

Equilibrium (1) corresponds to the requested de-solvation of the partners. It is obviously characterized by $\Delta H_1 > 0$ and $\Delta S_1 > 0$, which produces a compensation effect in the global free energy $\Delta G_1 = \Delta H_1 - T\Delta S_1$. It is worth noting that, when Solv = H_2O, these enthalpic and entropic contributions are often comparable and $\Delta G_1 \approx 0$.[15] Equilibrium (2) refers to a simple association process, for which $\Delta H_2 < 0$ and $\Delta S_2 < 0$. The latter entropic term strongly depends on charge compensation effects and it becomes less negative when the negative charge of the ligand increases.[16] Altogether, both the global enthalpic $\Delta H_c = \Delta H_1 + \Delta H_2$ and entropic $\Delta S_c = \Delta S_1 + \Delta S_2$ changes during the complexation process contain opposite components, while the free energy $\Delta G_c = \Delta G_1 + \Delta G_2$ can be reduced to $\Delta G_c \approx \Delta G_2$ in water, the most used solvent for investigating complexation processes with such highly charged

Bertrand Donnio

Bertrand Donnio graduated in chemistry in 1991 from the University of Rennes (Bretagne, France) and obtained his PhD in 1996 from Sheffield University (UK) under the supervision of Professor D. W. Bruce. He then moved to Neuchâtel at the Institut de Chimie (Switzerland) in the group of Professor R. Deschenaux, and then joined the group of Professor H. Finkelmann at the Institut für Makromolekulare Chemie (Freiburg, Germany) for two consecutive postdoctoral fellowships. Since 1999, he has been Chargé de Recherche (CNRS) at the IPCMS-GMO. His research interests are focused on liquid crystals having original molecular architectures (design and synthesis of dendrimers, metallomesogens, elastomers, bent mesogens, hybrid systems), and in the way these molecules self-organise within liquid crystalline mesophases using small and wide angle X-ray diffraction and dilatometry.

Daniel Guillon

Daniel Guillon received his PhD degree in Chemical Physics in 1976 from the Louis Pasteur University of Strasbourg (France). He is director of research at CNRS, presently deputy director of the Institute of Physics and Chemistry of Materials of Strasbourg (IPCMS) since 2002, and head of the organic materials group of the institute since 1989. His main interests include the description at the molecular level of the mesomorphic structures exhibited by low molecular weight and polymer materials, the study of self-organisation processes in supramolecular chemistry, the bottom-up approach of organic and hybrid nanomaterials, and the structure of thin organic films. He has been the Vice-President of the International Liquid Crystal Society since 2004.

This journal is © The Royal Society of Chemistry 2006

cations. Some valuable conclusions can be drawn from these thermodynamic considerations, which may be useful for molecular programming:

1) In water, we expect a slight increase of the stability constant along the lanthanide series, because ΔH_2 becomes more negative with decreasing ionic radii. This effect is known as the regular electrostatic trend.[15]

2) For negatively charged ligands, the complexation reaction is dominated by a favorable entropic contribution since $\Delta S_1 \gg 0$, while ΔS_2 is only slightly negative due to the charge compensation effect.[16] On the other hand, $|\Delta H_1|$ is comparable with $|\Delta H_2|$ because they correspond to the formation, respectively the breaking of the same number of similar Ln–ligand bonds.[17]

3) For neutral ligands, the entropic balance is less favourable than for negatively charged ligands and both ΔH_c and ΔS_c contribute significantly to ΔG_c.

4) In less polar solvents with no oxygen donor atoms, such as organic media, the de-solvation process (eqn. (1)) is enthalpically much easier and the association step (eqn. (2)) becomes dominant, which opens attractive perspectives for using the standard concepts of pre-organization and pre-disposition, which specifically affect ΔH_2 and ΔS_2.[7,16] In thermotropic liquid crystals made up of neutral lanthanidomesogens [$LnLX_r$] (r = 0–3 depending on the charge borne by the ligand L, X being a monovalent counterion), it is preferable to avoid solvent molecules, which limits the thermodynamic analysis to two successive dissociation processes shown in equilibria (3) and (4):

$$[LnLX_r] \leftrightarrows [LnX_r]^{(3-r)+} + L^{(3-r)-} \quad (3)$$

$$[LnX_r]^{(3-r)+} + L^{(3-r)-} \leftrightarrows Ln^{3+} + rX^- + L^{(3-r)-} \quad (4)$$

Equilibrium (3) simply corresponds to the inverse of equilibrium (2), with $\Delta H_3 > 0$ and $\Delta S_3 > 0$. Equilibrium (4) is unlikely to occur for r = 2, 3, because of its considerable enthalpic cost ($\Delta H_4 \gg 0$) and of its limited entropic gain ($\Delta S_4 \geqslant 0$) resulting from the production of ions displaying opposite charges.

Therefore, lanthanidomesogens are mainly prone to an entropically-driven dissociation (eq. (3)) occurring at high temperature and the programming of thermotropic mesophases at the lowest possible temperature is a major challenge. A logical solution to overcome this limitation relies on the use of negatively charged ligands (r = 0, 1), for which the enthalpic contribution ΔH_3 is very large, while the entropic gain ΔS_3 is small. It is thus not so surprising that the first thermotropic lanthanide-containing mesophases have been evidenced for the neutral sandwich complexes [Ln(L*i*-2H)$_2$] (i = 1–5, hexagonal columnar, Col_h in the 20–250 °C range, Fig. 1), in which negatively charged phthalocyanines are coordinated to Ln^{III}.[4,18]

Concomitantly, much attention has been focused on the alternative lamellar organization produced by rod-like [Ln(L6)$_3$X$_3$] complexes (X = NO_3, $O_3SOC_{12}H_{25}$, Cl; Fig. 2).[4,10,19] Several different degrees of protonation for the ligands have been proposed, together with variable coordination spheres and donor atoms, until the X-ray crystal structures of low-molecular weight analogues showed that a specific zwitterionic hydroxy-imine form was responsible for the efficient monodentate complexation of L6 to Ln^{III}.[10c,20]

Since then, a large number of variations based on these two basic structures (*i.e.* neutral disk-like sandwich or rod-like complexes) have been reported,[4] among which it is worth noting (i) the addition of one lateral alkyl chain in L7, which transforms the layered organization (S_A) observed for [Ln(L6)$_3$X$_3$] into a hexagonal columnar arrangement (Col_h) in [Ln(L7)$_2$(L7-H)(CF_3SO_3)$_2$],[11] (ii) the use of β-diketonate as counterions in [Ln(L6a)$_2$(β-diketonate)$_3$][21] and (iii) the replacement of alkoxy-substituted phthalocyanines with related

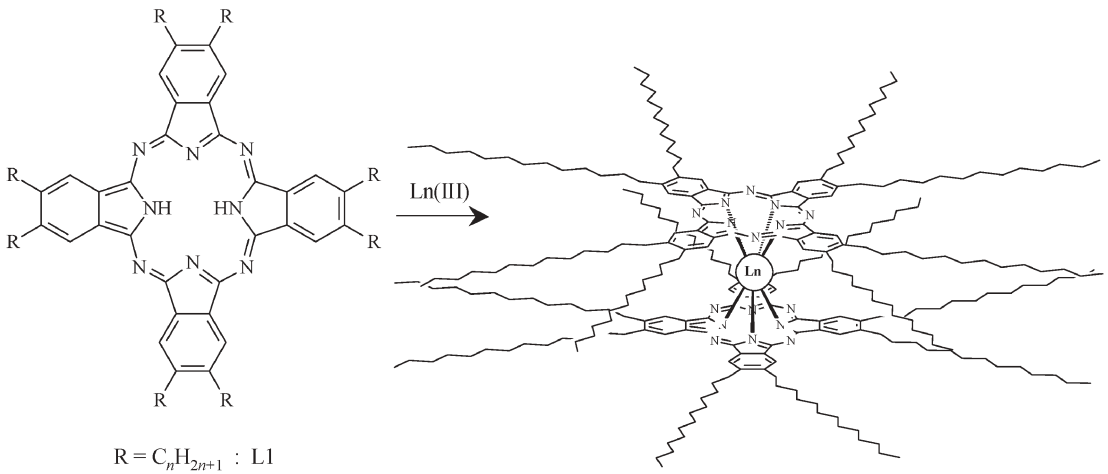

R = C_nH_{2n+1} : L1
R = $CH_2OC_nH_{2n+1}$: L2
R = OC_nH_{2n+1} : L3
R = SC_nH_{2n+1} : L4
R = $(OCH_2CH_2)_nCH_3$: L5

[Ln(L*i*-2H)$_2$]

Fig. 1 Syntheses of some disk-like sandwich lanthanidomesogens [Ln(L*i*-2H)$_2$] with phthalocyanine ligands (i = 1–5).

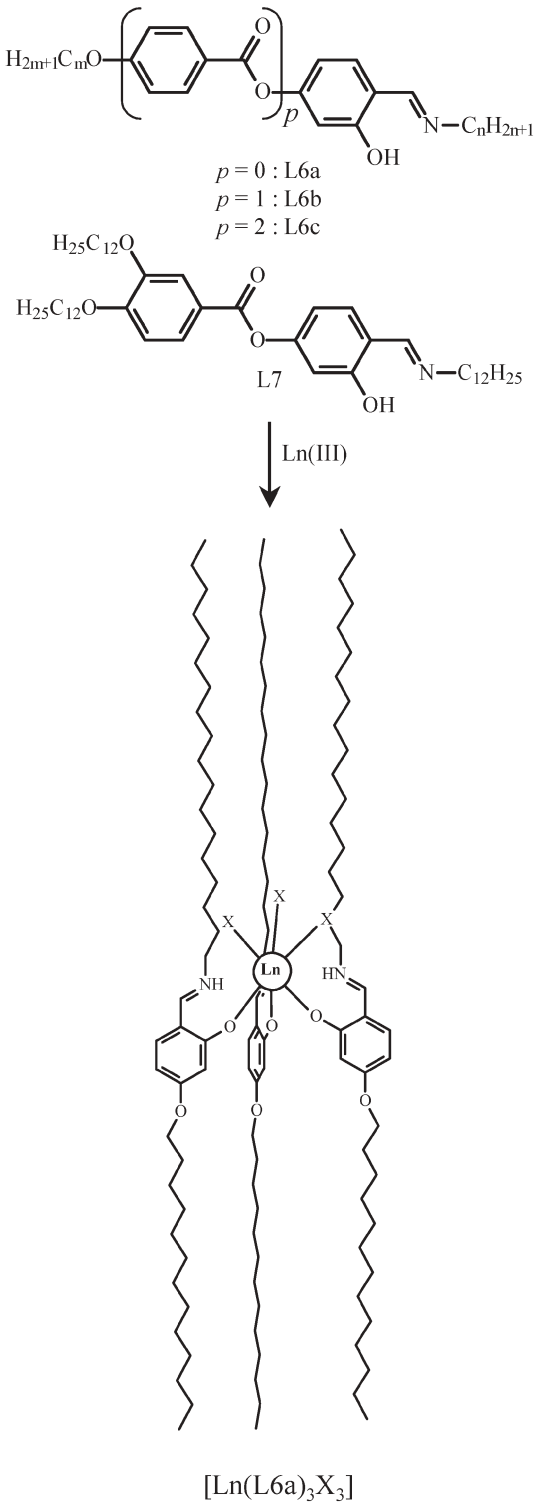

Fig. 2 Synthesis of the rod-like lanthanidomesogens $[Ln(Li)_3X_3]$ (i = 6, 7; X = NO_3, $O_3SOC_{12}H_{25}$, Cl, CF_3SO_3).

porphyrins (Por^{2-}) to give triple-decker $[Ce_2(Por)_3]$ complexes, in which the mesoscopic organization can be switched between columnar and lamellar forms depending on the chain lengths.[22] It is only recently, that the coordination of standard neutral chelating bidentate and tridentate ligands to Ln^{III} has been shown to be compatible with thermotropic mesomorphism in the complexes [Ln(L8)(β-diketonate)$_3$],[23] {Ln[M(Li-2H)]$_2$(NO$_3$)$_3$} (i = 9, 10; M = Ni^{II}, Cu^{II}),[12] [Ln(Li)(NO$_3$)$_3$] (i = 11, 12)[8] and $[Ln_2(L13)_2]$[13] (Fig. 3).

The beneficial entropic polycatenar effect resulting from the divergent connection of several alkyl chains to the rigid aromatic cores in the latter complexes (see Section 3), induces melting temperatures low enough to avoid dissociation in the mesophases according to eqn. (3). However, any depletion of the strength of the Ln–Li bond is deleterious for stability in the mesophase, as demonstrated by the use of trifluoroacetate counter-ions in [Ln(Li)(CF$_3$CO$_2$)$_3$] (i = 11, 12). Under these conditions, the small entropic cost ΔH_3 is overcome by $T\Delta S_3$ at low temperature, and dissociation is systematically observed in the mesophases.[24] It is thus surprising that despite its expected favourable contribution to ΔH_3 there is a single report on the use of a pre-organized neutral macrocyclic ligand decorated with long alkyl chains in [Ln(L14)(NO$_3$)$_3$] for designing stable lanthanidomesogens (Fig. 4).[9]

3. Melting, isotropisation, and organization in thermotropic mesophases

Let us remind here the thermodynamic definition of the standard melting temperature of a solid, as the temperature T_m at which the chemical potentials of the pure solid and of the pure liquid are equal under a fixed external pressure.[25] In common chemical terms, the free energy change of the melting process (ΔG_m) is thus given by $\Delta G_m = G_{(l)} - G_{(s)} = \Delta H_m - T_m\Delta S_m = 0$ (ΔH_m and ΔS_m are the melting enthalpy and entropy, respectively), and the coexistence of the two phases only results from the additional mixing entropy. We can therefore easily deduce that $T_m = \Delta H_m/\Delta S_m$, which is a valuable relationship for programming the formation of thermotropic mesophases, *i.e.* phases occurring from the melting of the solid, but separated from the isotropic liquid by a second melting process. In most thermotropic liquid crystals, such double melting processes arise from the presence of two incompatible parts in the molecule (*i.e.* an amphipathic molecule, not restricted to solely amphiphilic system),[26] which results from the connection of one or more long, flexible and poorly polarizable saturated hydrocarbon chains to rigid, and highly polarizable polyaromatic cores.[27] In simple cases, the minimum energy in the crystalline phase corresponds to a micro-segregated organization, which maximizes the dominant intermolecular multipolar electrostatic interactions between the polarizable aromatic cores, while the full extended hydrocarbon chains fill the voids, as illustrated in Fig. 5a for the rod-like ligand L15.[5a] Two concomitant enthalpic contributions are responsible for the cohesion of these amphipathic molecules in the solid state. The major stabilisation results from the intermolecular transient and static multipolar electrostatic attractions involving the polarizable aromatic cores, while a smaller contribution arises from the packing of the less polarizable alkyl chains. Conversely, the entropic gain upon melting is larger for the flexible alkyl chains than for the aromatic rigid cores.[14] Consequently, a simplistic and chemically intuitive thermodynamic model for the melting processes occurring in amphipathic molecules relies on the partial decoupling of the thermal behaviour of the packed alkyl

 This journal is © The Royal Society of Chemistry 2006

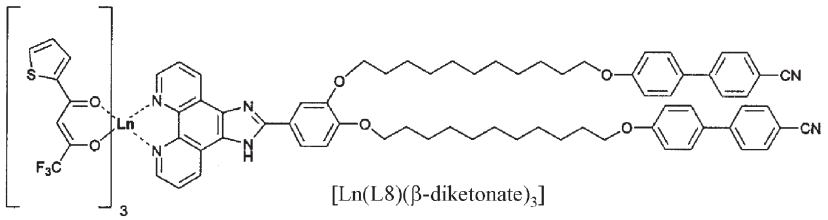

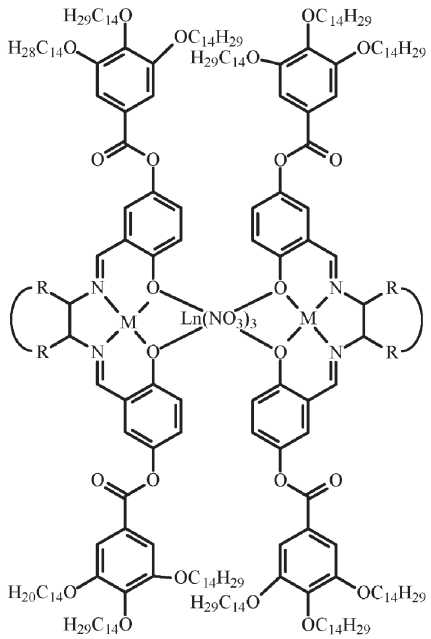

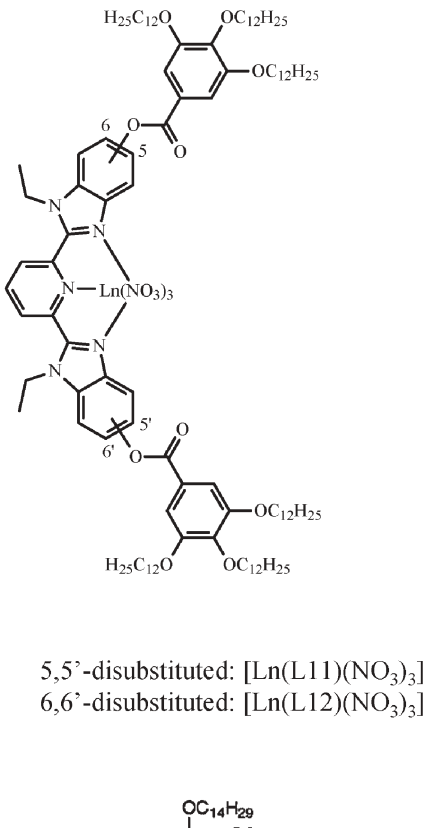

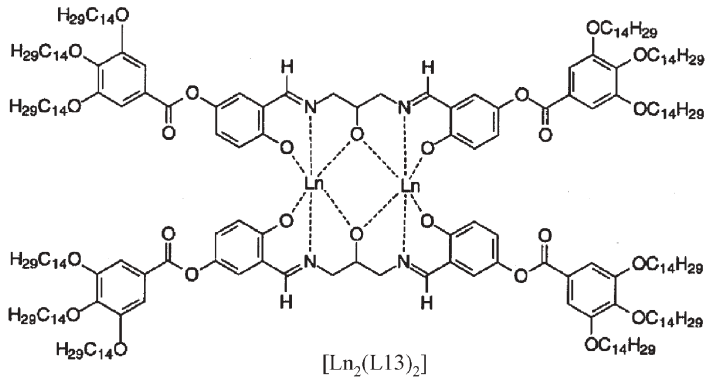

Fig. 3 Schematic structures of the lanthanidomesogens [Ln(L8)(β-diketonate)$_3$],[23] {Ln[M(L*i*-2H)]$_2$(NO$_3$)$_3$} (*i* = 9, 10; M = Ni^{II}, Cu^{II}),[12] [Ln(L*i*)(NO$_3$)$_3$] (*i* = 11, 12),[8] and [Ln$_2$(L13)$_2$].[13]

chains on one side (ΔH_m^{chains}, ΔS_m^{chains}) and of the stacked rigid cores (ΔH_m^{cores}, ΔS_m^{cores}) in the micro-segregated solid. Upon increasing the temperature $\Delta G_m^{chains} = \Delta H_m^{chains} - T_m^{chains}\Delta S_m^{chains} = 0$ is reached at lower temperature than $\Delta G_m^{cores} = \Delta H_m^{cores} - T_m^{cores}\Delta S_m^{cores} = 0$ (*i.e.*, $T_m^{chains} < T_m^{cores}$), because we expect $\Delta H_m^{chains} < \Delta H_m^{cores}$ and $\Delta S_m^{chains} > \Delta S_m^{cores}$ from the above discussion. A thermotropic liquid crystalline phase is thus formed between these two limits known as the melting $T_m = T_m^{chains}$ and clearing $T_c = T_m^{cores}$ temperatures. For chemists, a thermotropic mesophase can be thus roughly thought as a state of matter made up of clusters of packed semi-organized rigid cores dispersed in a continuum of the molten paraffinic chains. Such successive phase transitions are illustrated for ligand L15 in Fig. 5b. We immediately notice that the proposed entropic trend $\Delta S_m > \Delta S_c$, reminiscent of $\Delta S_m^{chains} > \Delta S_m^{cores}$, is obeyed, but the enthalpic counterpart is

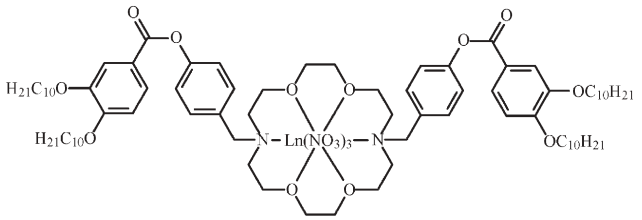

Fig. 4 Schematic structure of the macrocyclic lanthanidomesogens $[Ln(L14)(NO_3)_3]$.[9]

inverted with $\Delta H_m > \Delta H_c$ instead of the expected increases $\Delta H_m^{chains} < \Delta H_m^{cores}$. An obvious explanation may invoke the relative size of the appended semi-flexible dodecyloxybenzoic acid side chains (2 CH_3 + 24 CH_2 + 2 phenyl rings (8CH + 4 C) + 4 oxygen atoms) with respect to that of the rigid tridentate core (2 CH_3 + 2 CH_2 + 9 CH + 10 C + 5 N atoms, Fig. 5c).

Interestingly, the latter enthalpic behaviour $\Delta H_m > \Delta H_c$ is very common in thermotropic liquid crystals, which reflects the debatable strict decoupling of the phase transitions mainly associated with the specific melting of the different parts of the molecule. Our simplistic model must thus consider the melting process (lowest transition, T_m) as essentially reflecting the melting of the alkyl chains combined with a considerable decorrelation of the rigid cores, which is responsible for the fluidity of the mesophases. The clearing temperature (highest transition temperature, T_c) thus refers to the melting of the remaining residual clusters containing the polarizable rigid aromatic groups. An obvious consequence of this incomplete decoupling implies that both melting and clearing temperatures are influenced by the chemical nature of the rigid core. This rationalization also holds for the related organic ligands L11, L16 and L17 (Fig. 6), which further illustrate some additional and more subtle structural and thermodynamic parameters.

Fig. 6a shows that the extension of the central aromatic core indeed increases the enthalpic cost of the melting process, without significantly affecting the entropic release, thus leading to higher transition temperatures.[5b] Fig. 6b points to the crucial effect of the global molecular anisometry on both mesoscopic organization (a columnar phase is obtained for the V-shape ligand L17 instead of the layered smectic behaviour observed for the isomer L16), and on the thermodynamic of intermolecular interactions.[5c] Finally, Fig. 6c illustrates the beneficial effect of polycatenar systems (*i.e.* molecules decorated with a large number of diverging flexible alkyl chains). The considerable entropic cost associated with the crystallization (or at least the solidification) of six flexible alkyl chains is so high that no first-order melting transition can be detected with differential scanning calorimetry (DSC). We only observe a glassy transition by polarized light microscopy (PLM) followed by a standard clearing process.[8] Since glass transitions are kinetically controlled, they cannot match our simple thermodynamic model, and crystallization occurring over a longer period of time (> one year) cannot be excluded. However, whatever the kinetics or thermodynamic control, the entropic barrier remains the dominant contribution either to the activation free energy, or to the state free energies,

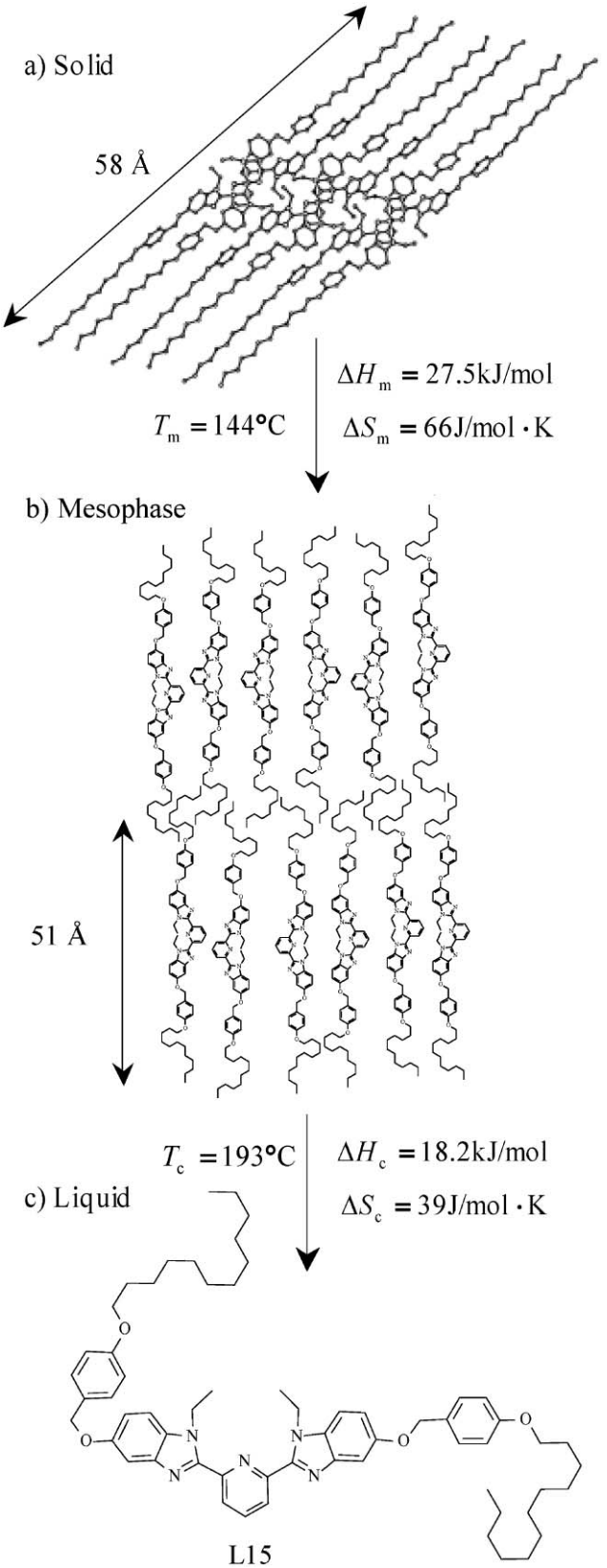

Fig. 5 The double melting process evidenced for ligand L15.[5a] a) X-ray crystal structure in the solid state. b) Organization in the smectic A (SmA) mesophase deduced from small-angle X-ray scattering (SAXS) patterns. c) Chemical structure of L15; the selected conformation aims at illustrating the large number of degrees of freedom of the ligand in the isotropic liquid. Reproduced with permission from ref. 14. Copyright Wiley-VCH 2006.

This journal is © The Royal Society of Chemistry 2006

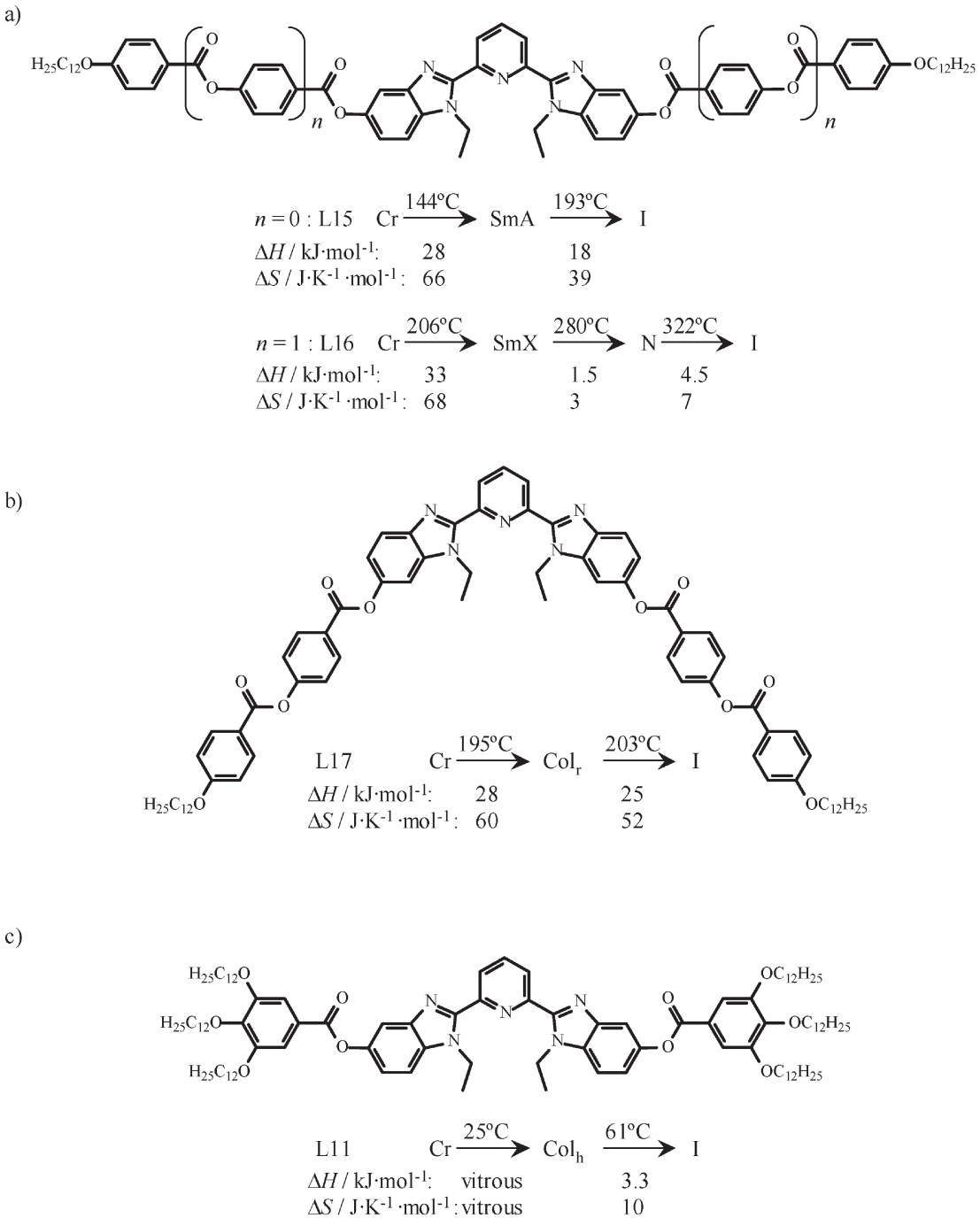

Fig. 6 Mesomorphic behaviour of the mesogenic ligands L11, L15–L17.[5,8] Illustration of the influence of a) the length of the spacer, b) the anisometry of the molecule and c) the number of flexible alkyl chains. (Cr: crystal, SmA: smectic A, SmX: undetermined smectic phase, N: nematic, Col_r: rectangular columnar, Col_h: hexagonal columnar, I: isotropic liquid.)

respectively. Consequently, the polycatenar ligand L11 provides liquid crystalline behaviour around room temperature. If we now focus on some structural predictions of the mesoscopic organization in the mesophase, it is sufficient to consider the curvature of the molecular interface separating the polarizable rigid core from the molten alkyl chains. The ratio $q_v = V_{alkyl}/V_{core}$ is considered as the crucial parameter for quantitatively measuring the curvature of the molecular interface (V_{alkyl} represents the volume of the alkyl chains, and V_{core}, that of the rigid core).[28] Obviously, a specific relationship with the geometry of the interface relies on the ratios q_S between the surfaces of the aromatic core and that of the connected flexible chains, a value which can deviate from q_v used in this review. However, for amphipathic molecules with comparable core and chain lengths, q_v and q_S follow the same trend, but q_v is often easier to obtain and it is more useful when a quantitative treatment of the multipolar electrostatic interactions is envisioned.

When the amphipathic molecules exhibit rod-like anisometry with the flexible alkyl chains connected to one or two circular faces of the molecular cylinders (*i.e.*, parallel to the molecular axis), $q \approx 1$ (typically $0.6 \leqslant q_v \leqslant 1.4$) and a flat interface develops between the two incompatible parts of the molecules (Fig. 7a). After entering the thermotropic mesophase at T_m, the disordered molten alkyl chains prevent intermolecular packing involving the surfaces to which they are connected (*i.e.* the circular faces of the cylinders in this case). Consequently, only intermolecular interactions perpendicular to the main molecular axis develop, and nematic and smectic mesomorphism occur, depending on the strength of the lateral intermolecular cohesion forces (Fig. 7a). When these peripheral interactions remain weak, one degree of orientational order ($\vec{n}$) is induced, which corresponds to the nematic organization (N), the lowest level of macroscopic organization. Conversely, when the peripheral interactions between the cylindrical rigid cores become significant, the orientational order is completed with a partial positional ordering, and layered smectic organization results (SmX, X = A for $\vec{n}$ perpendicular to the layers and X = C for $\vec{n}$ tilted with respect to the layers).[29] The thermotropic behaviour of ligands L15 and L16 (Fig. 6a) illustrates these predictions, since the connection of two dodecyloxy chains to the termini of the rod-like cores produces smectic behaviour at 'low' temperature (SmX), followed by nematic (N) organization at higher temperature resulting from the increased Brownian motion, which further limits lateral intermolecular cohesion.[5a] When a larger number of flexible chains are attached to the rigid core, divergent orientation results and $q_v > 1.5$, which produces a bent two-dimensional interface between the polarizable part and the chains (Fig. 7b). Intermolecular interactions then operate along a single, preferred direction, which coincides with the axis of the (supra)molecular discs (Fig. 7b).[30] Consequently, the molecules pack on top of each others and one degree of orientational order ($\vec{n}$) is observed in nematic discotic phases (N_D), when the intermolecular cohesion is weak. However, stronger intermolecular interactions introduce additional positional ordering, and columns are formed with different relative arrangements (hexagonal (Col_h), rectangular (Col_r) or oblique (Col_o) columnar).[29] These simplistic predictions justify the hexagonal columnar organization (Col_h) found in the mesophase of ligand L11 (Fig. 6c), which is induced by the divergent connection of the three dodecyloxy chains to each terminal gallic acid residue, a well-known behaviour in polycatenar systems.[30,31] Interestingly, special geometries of the rigid core may also dramatically affect these predictions and the V-shaped ligand L12, a geometrical isomer of the mesogenic I-shaped ligand L11 (Fig. 3) displays no mesomorphism, while the related extended V-shaped ligand L17 (Fig. 6b), which possesses only two divergent chains, evidences a Col_r mesophase at high temperature. Finally, a further increase of the curvature of the molecular interface ($q_v \gg 1.5$) eventually produces a three-dimensional arrangement of

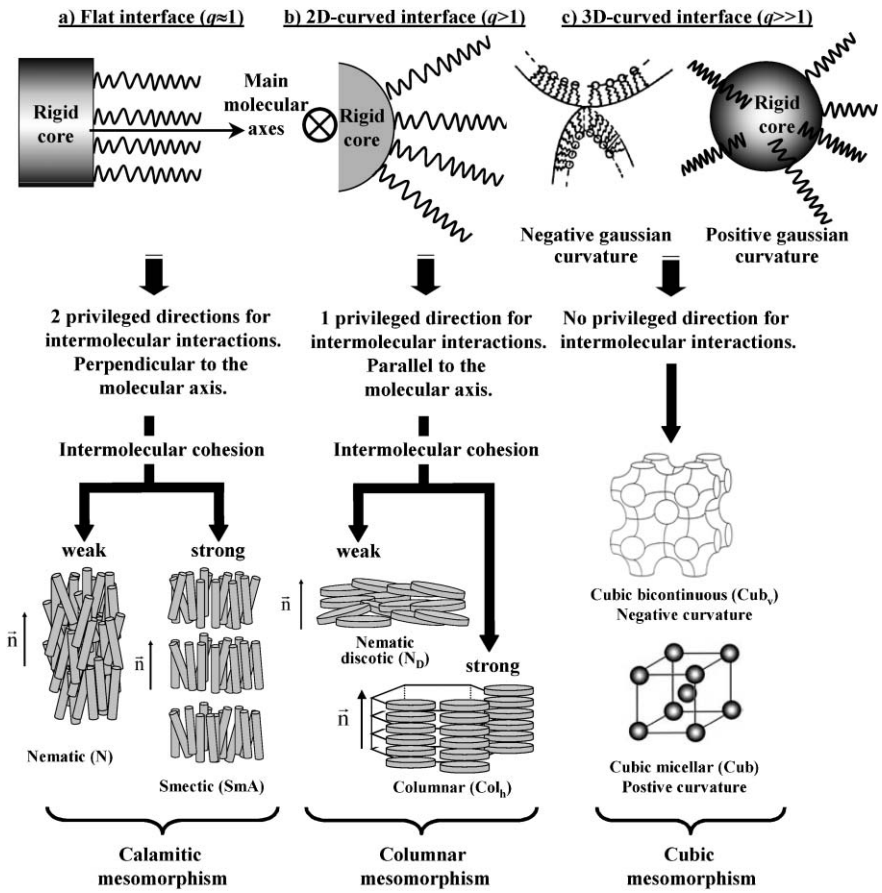

Fig. 7 Correlations between the geometry of the molecular interfaces separating the incompatible parts of the amphipathic molecules, and the resulting macroscopic organizations.

 This journal is © The Royal Society of Chemistry 2006

the flexible chains around the rigid core, which prevents any preferred direction for intermolecular interactions, and the micro-segregation process provides micellar cubic mesophases, or results in the complete suppression of mesomorphism (Fig. 7c).[28,32]

4. Bulky lanthanide cores in thermotropic liquid crystals: the lanthanidomesogens

The balance between the necessary entropically-driven melting of the alkyl chains ($\Delta S_m^{chains} \gg 0$) and the enthalpically-driven residual organization in the mesophase associated with sizeable intermolecular interactions between the rigid cores has led to the emergence of two optimum molecular anisometries, categorized as rod-like or disk-like geometries (see Section 3). The ligands L1–L17 systematically match one of these criteria and some predictive programming has become available. However, the introduction of bulky trivalent lanthanides Ln^{III} with high coordination numbers within the rigid core is expected to drastically alter molecular anisometry, thus leading to a considerable reduction in the core enthalpy ΔH_m^{cores}. Concomitantly, $T_c = \Delta H_m^{cores}/\Delta S_m^{cores}$ decreases and the domain of existence of the mesophases ($T_m <$ mesophase $< T_c$) shrinks to such an extent that no liquid crystalline behaviour could be detected for the complexes $[Ln(Li)(NO_3)_3]$ (i = 15–17).[5] In order to limit the deleterious effects of the expansion of the rigid core produced by its complexation to Ln^{III}, three attractive solutions have been proposed:

1) A spherical Ln^{III} ion, or its neutral salts LnX_3, can be encapsulated within large cavities produced by pro-mesogenic ligands, whose external surfaces remain compatible with standard rod-like or disk-like anisometry. The disk-like sandwich phthalocyanines $[Ln(Li\text{-}2H)_2]$ (i = 1–5, Fig. 1)[4,18] and the rod-like cylindrical $[Ln(L6)_3X_3]$ complexes (Fig. 2)[4,10] obey this concept and produce the expected thermotropic columnar (Col_h) and smectic (SmA) mesophases, respectively. If we now invoke the curvature of the molecular interface, its increase, in going from L6 to L7, induces columnar mesomorphism for $[Ln(L7)_2(L7\text{-}H)(CF_3SO_3)_2]$,[11] while its decrease in going from Li (i = 1–5) to the less substituted porphyrins in $[Ce_2(Por)_3]$ transforms columnar into lamellar organizations.[22]

2) Inspired by the remarkable incorporation of bulky fullerenes[33] or octasilsesquioxane[34] into thermotropic mesophases, Donnio, Binnemans and co-workers recently separated the bulky [Ln(β-diketonate)$_3$] unit from the rigid mesogenic cyanobiphenyl rigid cores in [Ln(L8)(β-diketonate)$_3$] (Fig. 3). The amphipathic character of the undecyloxy-cyanobiphenyl building blocks is only marginally affected, thus leading to the first report of well-characterized fluid nematic lanthanidomesogens (81–138 °C range).[23]

3) The last strategy relies on the connection of a sufficiently large amount of flexible alkyl chains to the bulky Ln^{III}-centred cores in order to maximise ΔS_m^{chains} and, consequently, to reduce $T_m = \Delta H_m^{chains}/\Delta S_m^{chains}$ to such an extent that a thermotropic liquid crystalline phase develops at low temperature. Since $q > 1.5$, the columnar mesophases observed for the tabular disk-like complexes $\{Ln[M(Li\text{-}2H)]_2(NO_3)_3\}$ (i = 9, 10; M = Ni^{II}, Cu^{II}),[12] $[Ln_2(L13)_2]$[13] (Fig. 3) and $[Ln(L14)(NO_3)_3]$ (Fig. 4)[9] are the logical result of the divergent connection of four to six flexible hydrocarbon chains to each aromatic ligand. Interestingly, only minor modifications of the transition temperatures due to the contraction of ionic radius are usually observed along the La–Lu series, except for $[Ln(L6a)_3(NO_3)_3]$, for which the domain of existence of the smectic phase (SmA) shrinks from Cr $\xrightarrow{83^\circ C}$ SmA $\xrightarrow{165^\circ C}$ I for Ln = La (*i.e.* the largest lanthanide ion) to Cr $\xrightarrow{135^\circ C}$ SmA $\xrightarrow{139^\circ C}$ I for Ln = Lu (*i.e.* the smallest lanthanide ion).[4,10] However the same lamellar mesoscopic organization is maintained for all complexes. The situation is completely different for the mesogenic hexacatenar complexes $[Ln(Li)(NO_3)_3]$, which display either hemi-disk-like (i = 11) or phasmidic (i = 12) geometries.[8] Both types of complexes exhibit an extreme dependence of the mesoscopic organization on the ionic size of Ln^{III} along the series. Let us focus on the hemi-disk-like complexes $[Ln(L11)(NO_3)_3]$ illustrated in Fig. 8, which display lamellar organization for the larger lanthanides (Ln = La–Nd), cubic mesophases for mid-range Ln = Sm–Ho, and hexagonal columnar organization for small Ln = Er–Lu.[8] For the latter complexes with Ln = Er–Lu, the limited expansion perpendicular to the aromatic 2,6-bis(benzimidazole)pyridine binding units produced by the $Ln(NO_3)_3$ core, allows efficient head-to-tail packing of the hemi-disk-like complexes, and hexagonal columnar organization (Fig. 8 right). When the size of the metal increases for mid-range lanthanides (Ln = Sm–Ho), the intermolecular intra-columnar packing is severely reduced, while residual inter-columnar interactions involving orthogonal gallic acid pairs are not affected. Competition between intra- and inter-columnar interactions operates, and either 'oscillation'[28b] or 'puckering'[35] of the columns is likely to result. In the former situation, the formation of dislocation points eventually leads to the isotropic growth of the columns in the three Cartesian directors of space, and thus a bi-continuous structure evolves.[36] In the latter case, the cylindrical rods are pinched off, and discrete micelles are formed. The three-dimensional close packing of these micelles, driven by the maximum occupancy of the available space, leads to a micellar cubic phase (see centre of Fig. 8). The differentiation between these two descriptions of the cubic organization is rarely unambiguous, and an intermediate interpretation with a maximum of electronic density located around the special positions of the cubic networks, together with residual electronic density in between, can be reasonably proposed (perhaps partially fused micelles). For larger lanthanides (Ln = La–Nd), the nine donor atoms provided by the three bidentate nitrate counter-ions (6 O atoms) and the 2,6-bis(benzimidazole)pyridine binding unit (3 N atoms) do not fill the coordination sphere. An enthalpy-driven dimerization occurs for producing ten-coordinate homobimetallic complexes containing two bridging nitrate anions:

$$2\ [Ln(L11)(NO_3)_3] \leftrightarrows [Ln(L11)(NO_3)_3]_2$$

The dimerization transforms hemi-disk-like into rod-like complexes with a reduced ratio q, which becomes close to $q \approx 1$.[8] Lamellar organization thus develops at low temperature, which is diagnostic for the existence of rod-like molecular dimers (Fig. 8, left). At higher temperature, the entropically-driven dissociation regenerates the hemi-disk-like

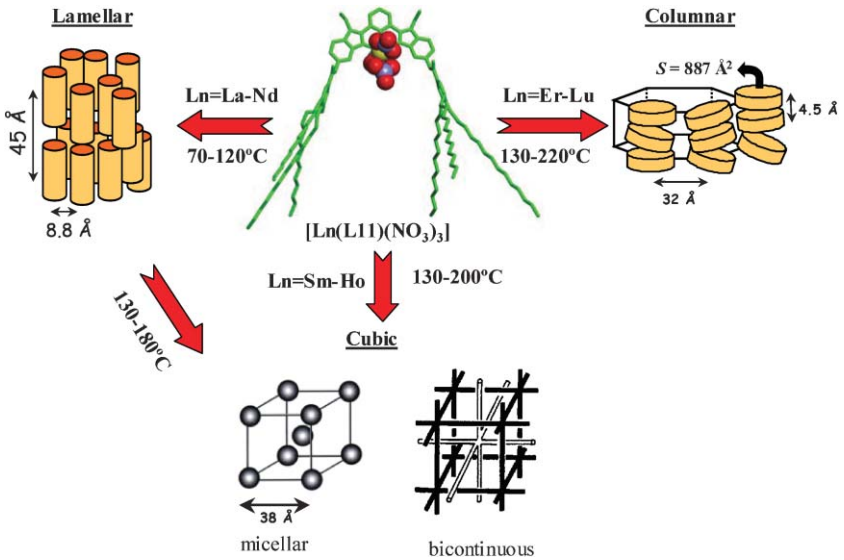

Fig. 8 Mesomorphic behaviour of the hemi-disk-like complexes $[Ln(L11)(NO_3)_3]$.

monomers and thus the cubic phases (Fig. 8, left). The isomeric phasmidic complexes $[Ln(L11)(NO_3)_3]$ display a very similar behaviour, except for an enthalpically more favourable dimerization process, which produces lamellar organization at low temperature along a considerable part of the lanthanide series (Ln = La–Ho).[8]

5. Exploiting lanthanide-centred optical properties in lanthanidomesogens

Probing the Ln^{III} microenvironment

The best known, and used, optical property of lanthanide ions concerns their ability to emit light since their absorption spectra have rather weak intensity due to the forbidden nature of f–f transitions, with molar absorption coefficients usually smaller than 3 M^{-1} cm^{-1}, except for a few transitions. Most of the Ln^{III} ions emit light, either by fluorescence or phosphorescence processes, and their emission lines span the UV, visible, and near-infrared (NIR) spectral ranges. Emission spectroscopy had been essential in the discovery of the elements in the 19th century; conversely the lanthanide ions have always played a prominent role in lighting applications and, more recently, in optics for telecommunications, as well as in biomedical analyses and imaging.[37] Insertion of Ln^{III} ions into molecular edifices results in the electronic levels (characterized by the quantum numbers S, L, and J) being split by (weak) ligand-field effects (LF). Transitions between (SLJ) levels are governed by selection rules which are somewhat relaxed in view of the mixing of either vibrational, ligand, or charge transfer states in the 4f wavefunctions, and of the spin–orbit coupling. On the other hand, transitions between LF sublevels are strictly governed by symmetry selection rules: a transition between Γ_J and $\Gamma_{J'}$ is only allowed if $\Gamma_{op} \in \Gamma_J \times \Gamma_{J'}$, that is if the product of the irreducible representations of the initial (J) and final (J') wavefunctions contains the irreducible representation of the dipolar operator (electric or magnetic). Therefore analysis of high-resolution luminescence spectra using group-theoretical considerations allows the determination of the ligand-field splitting of the levels and of the site symmetry of the Ln^{III} ion. The Eu^{III} ion is a particularly powerful luminescent probe since its major emitting state is the un-split level $^5D_0$, which simplifies the analysis, and this ion has been used to investigate its microenvironment. For instance, such an analysis has been conducted for the Eu^{III} complex depicted in Fig. 4 under its crystalline form and has shown that it contains two different chemical environments for Eu^{III}, the first one without coordinated water molecule having C_2 symmetry and a population of about ¾, whereas the second environment has a lower symmetry, a coordinated water molecule and a population of about ¼, in line with the chemical analysis.[38] Another point was to investigate if changes in the LF splitting and/or transition probabilities can be detected when the material undergoes a transition into the mesomorphic phase. This is a quite difficult problem to address in that the luminescence intensity diminishes with increasing temperature (see below) and thermal motions contribute to the broadening of the emission lines; moreover, most of the molecular lanthanidomesogens studied in our laboratories have relatively high transition temperatures so that no definitive information could be gathered. On the other hand, a similar experiment was attempted on a mesomorphic solution of europium nitrate 5 mol% in 1-dodecyl-3-methylimidazole chloride,[39] which undergoes a Cr → SmA_2 transition around 0 °C, while isotropisation occurs around 100 °C (the exact temperatures depend on the hydration of the samples).[40] Unambiguous variations have been observed, although they appear to develop more or less continuously, without a clear break at the transition temperatures.[39]

Determining the transition temperature by Eu^{III} (and Tb^{III}) luminescence

It is a well known fact that both the luminescence intensity (I_{obs}) and lifetime of the excited state (τ_{obs}) diminish with

 This journal is © The Royal Society of Chemistry 2006

increasing temperature because non-radiative de-excitation involves temperature-dependent vibrational and/or electronic processes. For the intensity, the expected variation is of the form $I_{obs} = I_0 e^{-\frac{C}{RT}}$, so that monotonous $\ln\frac{I_{obs}}{I_{295K}}$ curves are expected in absence of phase transition. When the investigated material undergoes a phase transition, the refractive index is known to display a sigmoid variation. From a theoretical point of view, the emission intensity I_{obs} of Ln^{III} ions is related to:

$$A(J,J') = \frac{64\pi^2\tilde{\nu}^3}{3h(2J+1)}\left[\frac{n(n^2+2)^2}{9}D_{ED} + n^3 D_{MD}\right] \quad (5)$$

in which $A(J, J')$, in s^{-1}, represents the Einstein probability of spontaneous emission, $\tilde{\nu}$ is the average energy of the transition (cm^{-1}), h is Planck's constant ($6.63\cdot10^{-27}$ erg s), $(2J + 1)$ is the degeneracy of the initial state (1 for $Eu(^5D_0)$), while D_{ED} and D_{MD} (in $esu^2\cdot cm^2$) are the contributions from the electric and magnetic dipole operators, respectively; and n is the refractive index of the medium.[41] The two expressions $n(n^2 + 2)^2/9$ and n^3 are known as the Lorentz correction factor for local electric field. Therefore S-shaped variation in I_{obs} is expected over the phase transition due to the n^5 polynomial expression given in eqn. (5). On the other hand, the lifetime of the excited state τ_{obs} is defined by the following expression:

$$\frac{1}{\tau_{obs}} = \frac{1}{\tau_{rad}} + \frac{1}{\tau_{nr}} = \frac{1}{A(J,J')} + \frac{1}{W_T(J)} \quad (6)$$

in which $W_T(J)$ is the temperature-dependent sum of the rate constants of all non-radiative processes.[41] For the part of this term implying non-radiative relaxation between LF energy levels, the rate is essentially determined by temperature, the energy gap, and the energy of the phonons implied, according to an "energy gap law". Therefore the τ_{obs} *vs* T dependence will be somewhat more complex than the I_{obs} dependence.

In the case of Eu^{III}, the transition most sensitive to changes in the environment of the metal ion is the hypersensitive $^5D_0 \rightarrow {}^7F_2$ transition, which is purely electric dipole in nature; as a consequence, the second term of eqn. (5) vanishes and grouping all the constants yields the simplified relationship, where cst is a proportionality constant:

$$I_{obs}(0,2) = \frac{n(n^2+2)^2}{9} \times D_{ED} \times \text{cst} \quad (7)$$

Experimental data for $[Eu(L14)(NO_3)_3]\cdot\frac{1}{4}H_2O$ (*cf.* Fig. 4) are reported on Fig. 9. The compound displays a phase transition to a hexagonal columnar phase Col_h at 86 °C according to DSC (Fig. 9a), PLM, and SAXS measurements. The change in luminescence intensity upon heating the sample displays a sigmoid curve, from which the transition temperature can be determined. Most of the observed difference at this temperature is genuine to the phase transition since the contribution from the S-shaped refractive index term in eqn. (7) amounts to at most 15% of the total variation (Fig. 9b). Moreover, the same experiments conducted on two non-mesomorphic reference compounds, europium nitrate and $[Eu(L14a)(NO_3)_3]$ in which the C_{10} alkyl chains in L14 are replaced by methyl groups in L14a, present a monotonous variation of the luminescence intensity *versus* temperature. The cooling curve presents a far less pronounced sigmoid variation, although, a second (and subsequent) heating(s) yields the same temperature dependence as initially observed. Similarly, an associated S-shape variation in the lifetime of the $^5D_0$ level *versus* temperature (both during heating and cooling) fully confirms the sensitivity of the luminescence parameters to the

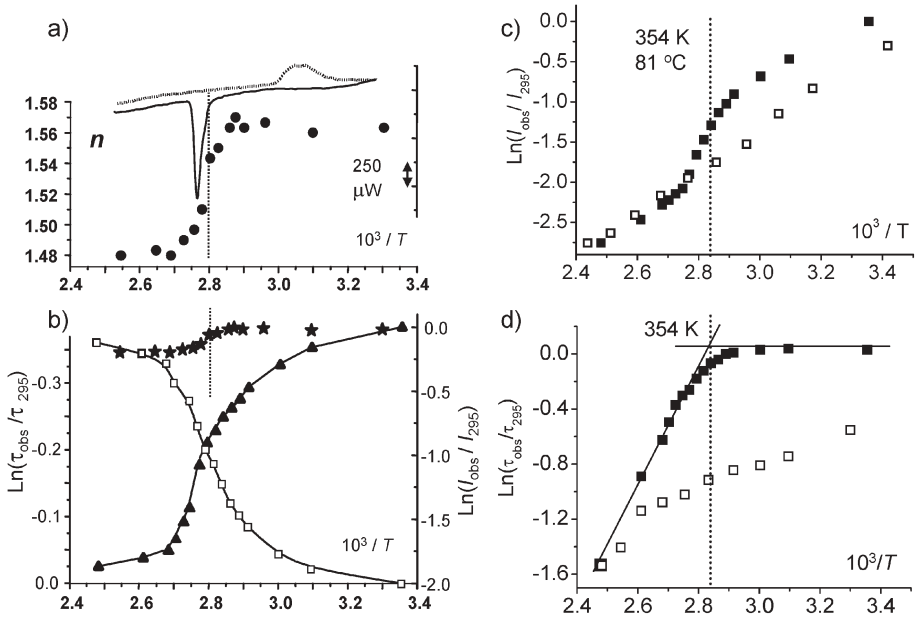

Fig. 9 Detection of the Cr → Col_h (and *vice-versa*) phase transition in $[Ln(L14)(NO_3)_3]$. Left, Ln = Eu, (a) DSC trace and refractive index variation, (b) luminescence parameter variation (▲, intensity; □, lifetime) with, at the same scale the contribution of the refractive index to the intensity change (*). Right, Ln = Tb, filled squares for the heating process, empty squares for the cooling process; (c) intensity change and (d), lifetime variation. Redrawn from ref. 37.

changes in the metal microenvironments during the melting process. The changes observed for $I(^5D_0 \rightarrow {}^7F_2)$ and τ are reversible and several heating-cooling cycles generate the same patterns, from which values for the temperature transition can be calculated, which fairly well match to one determined with the other experimental techniques.[38] A comparable effect has been observed for $[Tb(L14)(NO_3)_3]$, for which the intensity variation of the $^5D_4 \rightarrow {}^7F_5$ transition follows the same trend as that for the Eu^{III} compound (Fig. 9c). In this case, however, the $^5D_4$ lifetime remains constant up to the transition temperature and then $\ln(\tau_{obs}/\tau_{295})$ decreases linearly with $1/T$ (Fig. 9d), confirming what is said above with respect to eqn. (6).

Since luminescence data are easily collected, we have further tested whether or not this technique for the determination of the transition temperature is general and, if not, which are its limitations. The chosen system was $[Eu(L11)(NO_3)_3]$ (Fig. 3) since it displays a rich and varied mesomorphism.[8b] Sigmoid variations are seen for both logarithmic plots (intensity and lifetime) when the complex enters the cubic mesophase during the first heating process. A mathematical analysis of these curves gives $T = 413(2)$ K for the transition temperature, which exactly matches that found by the other experimental techniques. However, the following cooling process and subsequent heating-cooling cycles show that the Cub mesophase is supercooled in the final glassy state. As a result, no significant structural variation occurs during these subsequent phase transitions and both logarithmic plots become monotonous with temperature. As a conclusion, luminescence intensity and/or lifetime switching can be used to signal Cr-LC transitions in Eu^{III} and Tb^{III} mesomorphic compounds, but glass transitions are not accessible with this technique of detection.

Similar sharp variations at the transition temperature have been reported by Binnemans and co-workers. For instance, a two-fold increase in the metal-centred luminescence of the nematic liquid-crystalline matrix MBBA (N-4-methoxybenzylidene)-4-butylaniline) doped by $[Yb(dbm)_3(phen)]$ (dbm is dibenzoylmethanate and phen is *o*-phenanthroline) occurs in going from the isotropic phase (47 °C) to the nematic phase (12 °C); in this case, however, the result can be explained by the better scattering of the excitation light in the liquid-crystalline phase, as opposed to the isotropic liquid.[42] On the other hand, glass dispersed liquid crystal films of 5CB (4-pentyl-4′-cyanobiphenyl) doped with $[Eu(dbm)_3(dme)]$ (dme is 1,2-dimethoxyethane) show a strong intensity change at the nematic-to-isotropic transition, both on heating and cooling.[43]

Doped thermotropic liquid crystals

An alternative to designing lanthanidomesogens is to dope lanthanide salts and/or highly luminescent complexes (generally β-diketonates) into known mesomorphic phases. As a matter of fact it is the way that the first lanthanide-containing mesophase was obtained, by introducing an Eu^{III} β-diketonate dihydrate into cholesteric and nematic phases.[44] Replacing the water molecules by phenanthroline subsequently led to improved photophysical properties,[42,45] as well as the use of glass-dispersed phases.[43] Such a strategy allows one to tune the emission color of the liquid-crystalline phases by a judicious choice of the lanthanide ion, the receptor, and the excitation wavelength. Among the goals pursued by the researchers in this area is the design of strongly NIR-emitting liquid-crystalline phases. In view of their peculiar chemical and solvent properties, room temperature ionic liquids (RTILs) which are simultaneously liquid crystalline offer a large variety of possibilities. RTILs are usually comprised of a bulky organic cation and an inorganic anion and are presently receiving a wealth of attention because of their low volatility and potential as solvents for various ''green'' chemical processes. Their use as liquid crystals, as well as host for lanthanide-containing compounds has recently been reviewed.[46] In our laboratories, we have taken advantage of the mesogenic properties of 1-dodecyl-3-methylimidazolium chloride ($[C_{12}$-mim]Cl). This salt forms lamellar, sheet-like arrays in the crystalline phase and an enantiotropic smectic liquid crystalline phase at room temperature. Introduction of lanthanide salts into this ionic liquid does not alter much the liquid crystalline properties up to 10 mol%. The intrinsic quantum yield (*i.e.* the quantum yield obtained upon metal excitation) of the Eu^{III}-centred luminescence is large, in the range 52–61% depending on the anion. As a consequence, the emission color of the Eu^{III}-containing materials can be tuned from blue to red by varying the counterion and the excitation wavelength (Fig. 10), that is by tuning the mix between the blue RTIL emission and the red metal-centred luminescence. This opens interesting perspectives for the design of environmental-friendly luminescent devices.[47] The same RTIL has also been doped by 1 mol% of [Ln(tta)(phen)] (Ln = Nd, Eu, Er, Yb) complexes (tta is thenoyltrifluoroacetonate). Both DSC and SAXS measurements, as well as high-resolution luminescence spectroscopy on Eu^{III} confirm that the introduction of these complexes does not change the mesomorphic properties of the RTIL. Intense NIR emission is obtained with the Nd^{III}-, Er^{III}-, and Yb^{III}-doped phases. Emission is enhanced with respect to the initial complexes and the quantum yield of the Yb^{III}-doped phase reached $2.1 \pm 0.3\%$.[40]

6. Conclusions and outlook

The proposed simplistic thermodynamic approach responsible for phase transitions occurring in thermotropic organic liquid crystals, also applies for lanthanidomesogens, provided that the perturbation of the anisometry of the amphipathic molecule is carefully considered. For bulky lanthanide metals, the deleterious decrease of ΔH_m^{cores} can be overcome by using different strategies based on (i) the embedding of Ln^{III} within an internal coordination cavity, (ii) the decoupling of the lanthanide core from the polarizable aromatic core responsible for the emergence of ΔH_m^{cores}, and (iii) the connection of a large number of peripheral flexible alkyl chains to the rigid core in polycatenar complexes. All these approaches have been shown to successfully provide thermotropic mesophases with lanthanidomesogens, with a pronounced preference for columnar organization resulting from sizeable curvatures of the molecular interfaces ($q_v \gg 1$). Moreover, the large number of electrons brought by the lanthanide core contributes to an improved intermolecular cohesion based on transient

 This journal is © The Royal Society of Chemistry 2006

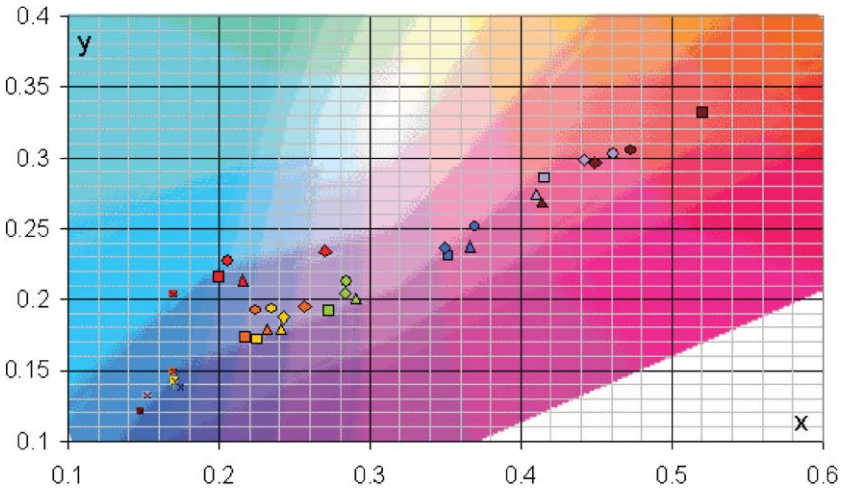

Fig. 10 Part of the trichromatic diagram displaying the position of [C_{12}-mim]Cl and Eu^{III}-containing samples (5 mol%) as a function of the nature of the anion (×: RTIL, ■: chloride, ◆: nitrate, ▲: triflate, ●: perchlorate) and the excitation wavelength (grey: 274 nm, violet: 285 nm, blue: 334 nm, green: 344 nm, yellow: 353 nm, orange: 361 nm, red: 393 nm). Reproduced with permission from ref. 46. Copyright 2004. American Chemical Society.

multipolar electrostatic interactions, and consequently ΔH_m globally increases, which produces unfavourable high melting and clearing temperatures. These two characteristics, *i.e.* highly organized mesophases produced at high temperature, are major limiting factors for designing luminescent liquid crystals with potential applications, since fluid room-temperature mesophases are eventually required. The recent preparation of fluid nematic mesophases at 80–90 °C with the complexes [Ln(L8)(β-diketonate)$_3$] is thus a crucial contribution to this field,[23] particularly when we consider the entropic limitation of the thermal stability of lanthanidomesogens. We can therefore anticipate that the design of novel nematic lanthanidomesogens with lower melting temperatures according to the decoupling approach will attract much attention in the near future. If we now consider the optical functions brought by trivalent lanthanides in mesophases, it is obvious that tuneable metal-centred emission (green for Tb^{III}, red for Eu^{III}, blue for Tm^{III} and Eu^{II}) will be a central point for further developments. Because no switchable room-temperature lanthanidomesogen is currently available, the preparation of organic liquid crystals doped with small amounts of luminescent lanthanides is attractive, but this situation could be reconsidered in the future. In this context, the design of chiral environments in lanthanidomesogens may have a great potential for (i) designing luminescent fast-switching ferroelectric mesophases and (ii) producing circularly polarized emission addressable by appropriate filtering techniques, thus leading to the temperature variation of the dissymmetry factors as a probe for phase transitions.[48]

Acknowledgements

We warmly thank the collaborators and co-workers who contributed to these projects. Their names are mentioned in the associated publications quoted in the references. Financial support from the Swiss National Science Foundation and the Swiss Office for Science and Education is gratefully acknowledged.

Notes and references

1 D. W. Bruce, *J. Chem. Soc., Dalton Trans.*, 1993, 2983.
2 (*a*) A. M. Giroud-Godquin and P. M. Maitlis, *Angew. Chem., Int. Ed. Engl.*, 1991, **30**, 375; (*b*) S. A. Hudson and P. M. Maitlis, *Chem. Rev.*, 1993, **93**, 861; (*c*) J. L. Serrano, *Metallomesogens, Synthesis, Properties and Applications*, VCH, Weinheim, 1996; (*d*) B. Donnio and D. W. Bruce, *Struct. Bonding*, 1999, **95**, 194; (*e*) B. Donnio, D. Guillon, R. Deschenaux and D. W. Bruce, in *Comprehensive Coordination Chemistry*, ed. J. A. McCleverty and T. J. Meyer, Elsevier, Oxford UK, 2003, Vol.7, Chapter 79, 357.
3 (*a*) K. Binnemans, B. Heinrich, D. Guillon and D. W. Bruce, *Liq. Cryst.*, 1999, **26**, 1717; (*b*) K. Binnemans, L. Jongen, C. Bromant, D. Hinz and G. Meyer, *Inorg. Chem.*, 2000, **39**, 5938; (*c*) L. Jongen, G. Meyer and K. Binnemans, *J. Alloys Compd.*, 2001, **323–324**, 142; (*d*) L. Jongen, D. Hinz, G. Meyer and K. Binnemans, *Chem. Mater.*, 2001, **13**, 2243; (*e*) L. Jongen, B. Goderis, I. Dolbnya and K. Binnemans, *Chem. Mater.*, 2003, **15**, 212; (*f*) H. Li, W. Bu, W. Qi and L. Wu, *J. Phys. Chem. B*, 2005, **109**, 21669.
4 K. Binnemans and C. Görller-Walrand, *Chem. Rev.*, 2002, **102**, 2303 and references therein.
5 (*a*) H. Nozary, C. Piguet, P. Tissot, G. Bernardinelli, J.-C. G. Bünzli, R. Deschenaux and D. Guillon, *J. Am. Chem. Soc.*, 1998, **120**, 12274; (*b*) H. Nozary, C. Piguet, J.-P. Rivera, P. Tissot, G. Bernardinelli, N. Vulliermet, J. Weber and J.-C. G. Bünzli, *Inorg. Chem.*, 2000, **39**, 5286; (*c*) H. Nozary, C. Piguet, J.-P. Rivera, P. Tissot, P.-Y. Morgantini, J. Weber, G. Bernardinelli, J.-C. G. Bünzli, R. Deschenaux, B. Donnio and D. Guillon, *Chem. Mater.*, 2002, **14**, 1075.
6 (*a*) D. W. Bruce and X.-H. Liu, *Liq. Cryst.*, 1995, **18**, 165; (*b*) X.-H. Liu, M. N. Abser and D. W. Bruce, *J. Organomet. Chem.*, 1998, **551**, 271; (*c*) K. E. Rowe and D. W. Bruce, *J. Chem. Soc., Dalton Trans.*, 1996, 3913; (*d*) H. Zheng and T. M. Swager, *J. Am. Chem. Soc.*, 1994, **116**, 761; (*e*) T. M. Swager and H. Zheng, *Mol. Cryst. Liq. Cryst.*, 1995, **260**, 301.
7 (*a*) C. Piguet and J.-C. G. Bünzli, *Chem. Soc. Rev.*, 1999, **28**, 347; (*b*) J.-C. G. Bünzli and C. Piguet, *Chem. Rev.*, 2002, **102**, 1897.
8 (*a*) E. Terazzi, J.-M. Bénech, J.-P. Rivera, G. Bernardinelli, B. Donnio, D. Guillon and C. Piguet, *Dalton Trans.*, 2003, 769; (*b*) E. Terazzi, S. Torelli, G. Bernardinelli, J.-P. Rivera, J.-M. Bénech, C. Bourgogne, B. Donnio, D. Guillon, D. Imbert, J.-C. G. Bünzli, A. Pinto, D. Jeannerat and C. Piguet, *J. Am. Chem. Soc.*, 2005, **127**, 888.
9 S. Suarez, O. Mamula, R. Scopelliti, B. Donnio, D. Guillon, E. Terazzi, C. Piguet and J.-C. G. Bünzli, *New J. Chem.*, 2005, **29**, 1323.
10 (*a*) Y. Galyametdinov, M. A. Athanassopoulou, K. Griesar, O. Kharitonova, E. A. Soto Bustamante, L. Tinchurina,

I. Ovchinnikov and W. Haase, *Chem. Mater.*, 1996, **8**, 922; (*b*) K. Binnemans, Y. G. Galymetdinov, S. R. Collinson and D. W. Bruce, *J. Mater. Chem.*, 1998, **8**, 1551; (*c*) K. Binnemans, Y. G. Galyametdinov, R. Van Deun, D. W. Bruce, S. R. Collinson, A. P. Polishchuk, I. Bikchantaev, W. Haase, A. V. Prosvirin, L. Tinchurina, U. Litvinov, A. Gubajdullin, A. Rakhmatullin, K. Uytterhoeven and L. Van Meervelt, *J. Am. Chem. Soc.*, 2000, **122**, 4335; (*d*) R. van Deun and K. Binnemans, *Liq. Cryst.*, 2001, **28**, 621; (*e*) Y. G. Galyametdinov, W. Haase, L. Malykhina, A. Prosvirin, I. Bikchantaev, A. Rakhmatullin and K. Binnemans, *Chem.–Eur. J.*, 2001, **7**, 99; (*f*) K. Binnemans, D. Moors, T. N. Parac-Vogt, R. van Deun, D. Hinz-Hübner and G. Meyer, *Liq. Cryst.*, 2002, **29**, 1209; (*g*) N. V. S. Rao, M. K. Paul, T. R. Rao and A. Prasad, *Liq. Cryst.*, 2002, **29**, 1243.

11 (*a*) K. Binnemans, D. W. Bruce, S. R. Collinson, R. van Deun, Yu. G. Galyametdinov and F. Martin, *Philos. Trans. R. Soc. London, Ser. A*, 1999, **357**, 3063; (*b*) F. Martin, S. R. Collinson and D. W. Bruce, *Liq. Cryst.*, 2000, **27**, 859.

12 (*a*) K. Binnemans, K. Lodewyckx, B. Donnio and D. Guillon, *Chem.–Eur. J.*, 2002, **8**, 1101; (*b*) K. Binnemans and K. Lodewyckx, *Supramol. Chem.*, 2003, **15**, 485; (*c*) K. Binnemans, K. Lodewyckx, B. Donnio and D. Guillon, *Eur. J. Inorg. Chem.*, 2005, 1506.

13 K. Binnemans, K. Lodewyckx, T. Cardinaels, T. N. Parac-Vogt, C. Bourgogne, D. Guillon and B. Donnio, *Eur. J. Inorg. Chem.*, 2006, 150.

14 E. Terazzi, S. Suarez, S. Torelli, H. Nozary, D. Imbert, O. Mamula, J.-P. Rivera, E. Guillet, J.-M. Bénech, G. Bernardinelli, R. Scopelliti, B. Donnio, D. Guillon, J.-C. G. Bünzli and C. Piguet, *Adv. Funct. Mater.*, 2006, **16**, 157.

15 G. R. Choppin, in *Lanthanide Probes in Life, Chemical and Earth Sciences: Theory and Practice*, ed. J.-C. G. Bünzli and G. R. Choppin, Elsevier, 1989, ch. 1.

16 R. J. Motekaitis, A. E. Martell and R. A. Hancock, *Coord. Chem. Rev.*, 1994, **133**, 39.

17 J.-M. Senegas, G. Bernardinelli, D. Imbert, J.-C. G. Bünzli, P.-Y. Morgantini, J. Weber and C. Piguet, *Inorg. Chem.*, 2003, **42**, 4680.

18 (*a*) C. Piechocki, J. Simon, J. J. André, D. Guillon, A. Skoulios and P. Weber, *Chem. Phys. Lett.*, 1985, **122**, 124; (*b*) T. Komatsu, K. Ohta, T. Fujimoto and I. Yamamoto, *J. Mater. Chem.*, 1994, **4**, 533; (*c*) T. Toupance, P. Bassoul, L. Mineau and J. Simon, *J. Phys. Chem.*, 1996, **100**, 11704; (*d*) K. Ban, K. Nishizawa, K. Ohta, A. van de Craats, J. M. Warman, I. Yamamoto and H. Shirai, *J. Mater. Chem.*, 2001, **11**, 321; (*e*) J. Sleven, C. Görller-Walrand and K. Binnemans, *Mater. Sci. Eng., C*, 2001, **C18**, 229; (*f*) F. Maeda, K. Hatsusaka, K. Ohta and M. Kimura, *J. Mater. Chem.*, 2003, **13**, 243; (*g*) K. Binnemans, J. Sleven, S. De Feyter, F. C. De Schryver, B. Donnio and D. Guillon, *Chem. Mater.*, 2003, **15**, 3930.

19 (*a*) I. V. Ovchinnikov, Y. G. Galyametdinov, G. I. Ivanova and L. M. Yagfarova, *Dokl. Akad. Nauk SSSR*, 1984, **276**, 126; (*b*) Y. G. Galyametdinov, I. V. Ovchinnikov, B. M. Bolotin, N. B. Etingen, G. I. Ivanova and L. M. Yagarova, *Izv. Akad. Nauk SSSR, Ser. Khim.*, 1984, 2379; (*c*) I. V. Ovchinnikov, Y. G. Galyametdinov and I. G. Bikchantaev, *Izv. Akad. Nauk, Ser. Fiz.*, 1989, **53**, 1870; (*d*) R. M. Galimov, I. G. Bikchantaev and I. V. Ovchinnikov, *Zh. Strukt. Khim.*, 1989, **30**, 65; (*e*) Y. G. Galyametdinov, D. Z. Zakieva and I. V. Ovchinnikov, *Izv. Akad. Nauk SSSR, Ser. Khim.*, 1986, 491.

20 L. Van Meervelt, K. Uytterhoeven, R. van Deun and K. Binnemans, *Z. Kristallogr.- New Cryst. Struct.*, 2003, **218**, 488.

21 (*a*) K. Binnemans and K. Lodewyckx, *Angew. Chem., Int. Ed.*, 2001, **40**, 242; (*b*) K. Binnemans, K. Lodewyckx, T. N. Parac-Vogt, R. van Deun, B. Goderis, B. Tinant, K. Van Hecke and L. Van Meervelt, *Eur. J. Inorg. Chem.*, 2003, 3028.

22 H. Miwa, N. Kobayashi, K. Bans and K. Ohta, *Bull. Chem. Soc. Jpn.*, 1999, **72**, 7219.

23 T. Cardinaels, K. Driesen, T. N. Parac-Vogt, B. Heinrich, C. Bourgogne, D. Guillon, B. Donnio and K. Binnemans, *Chem. Mater.*, 2005, **17**, 6589.

24 H. Nozary, L. Guénée, E. Terazzi, G. Bernardinelli, B. Donnio, D. Guillon and C. Piguet, *Inorg. Chem.*, 2006, **45**, 2989.

25 P. W. Atkins, *Physical Chemistry*, 5th edn, Oxford University Press, Oxford, 1994, pp. 184–186.

26 D. Guillon and A. Skoulios, *J. Phys.*, 1976, **37**, 797.

27 K. J. Toyne, in *Thermotropic Liquid Crystals*, ed. G. W. Gray, *Critical Reports on Applied Chemistry*, Wiley, Chichester, New York, Brisbane, Toronto, Singapore, 1987, vol. 22, p. 28.

28 (*a*) D. W. Bruce, *Acc. Chem. Res.*, 2000, **33**, 831; (*b*) B. Donnio, B. Heinrich, T. Gulik-Krzywicki, H. Delacroix, D. Guillon and D. W. Bruce, *Chem. Mater.*, 1997, **9**, 2951.

29 (*a*) H. Zheng, C. K. Lai and T. M. Swager, *Chem. Mater.*, 1994, **6**, 101; (*b*) C. Tschierske, *J. Mater. Chem.*, 2001, **11**, 2647; (*c*) R. W. Date, E. Fernandez Iglesias, K. E. Rowe, J. M. Elliott and D. W. Bruce, *Dalton Trans.*, 2003, 1914; (*d*) B. Donnio, B. Heinrich, H. Allouchi, J. Kain, S. Diele, D. Guillon and D. W. Bruce, *J. Am. Chem. Soc.*, 2004, **126**, 15258; (*e*) L. Gehringer, C. Bourgogne, D. Guillon and B. Donnio, *J. Am. Chem. Soc.*, 2004, **126**, 3856; (*f*) B. Donnio, J. Barberá, R. Giménez, D. Guillon, M. Marcos and J.-L. Serrano, *Macromolecules*, 2002, **35**, 370.

30 (*a*) J. Malthête, H. T. Nguyen and C. Destrade, *Liq. Cryst.*, 1993, **13**, 171; (*b*) H. T. Nguyen, C. Destrade and J. Malthête, *Adv. Mater.*, 1997, **9**, 375.

31 (*a*) B. Donnio and D. Bruce, *J. Chem. Soc., Dalton Trans.*, 1997, 2745; (*b*) B. Donnio and D. Bruce, *New J. Chem.*, 1999, 275.

32 (*a*) C. J. Tschierske, *J. Mater. Chem.*, 1998, **8**, 1845; (*b*) B. Donnio, K. E. Rowe, C. P. Roll and D. W. Bruce, *Mol. Cryst. Liq. Cryst.*, 1999, **332**, 383; (*c*) C. J. Tschierske, *Annu. Rep. Prog. Chem., Sect. C: Phys. Chem.*, 2001, **97**, 191; (*d*) S. Diele, *Curr. Opin. Colloid Interface Sci.*, 2002, **7**, 333; (*e*) M. Impéror-Clerc, *Curr. Opin. Colloid Interface Sci.*, 2005, **9**, 370.

33 (*a*) B. Dardel, D. Guillon, B. Heinrich and R. Deschenaux, *J. Mater. Chem.*, 2001, **11**, 2814; (*b*) R. Deschenaux and S. Campidelli, *Helv. Chim. Acta*, 2001, **84**, 589; (*c*) S. Campidelli, R. Deschenaux, J.-F. Eckert, D. Guillon and J.-F. Nierengarten, *Chem. Commun.*, 2002, 656.

34 (*a*) I. M. Saez and J. W. Goodby, *Liq. Cryst.*, 1999, **26**, 1101; (*b*) I. M. Saez and J. W. Goodby, *J. Mater. Chem.*, 2005, **15**, 26.

35 P. Sakya, J. M. Seddon, R. H. Templer, R. J. Mirkin and G. J. T. Tiddy, *Langmuir*, 1997, **13**, 3706.

36 J. M. Seddon and R. H. Templer, *Philos. Trans. R. Soc. London, Ser. A*, 1993, **344**, 377.

37 J.-C. G. Bünzli and C. Piguet, *Chem. Soc. Rev.*, 2005, **34**, 1048.

38 (*a*) S. Suárez, O. Mamula, D. Imbert, F. Gumy, C. Piguet and J.-C. G. Bünzli, *Chem. Commun.*, 2003, 1226; (*b*) S. Suárez, D. Imbert, F. Gumy, C. Piguet and J.-C. G. Bünzli, *Chem. Mater.*, 2004, **16**, 3257.

39 F. Gumy, J. Kocher and J.-C. G. Bünzli, unpublished results, 2006.

40 L. N. Puntus, K. J. Schenk and J.-C. G. Bünzli, *Eur. J. Inorg. Chem.*, 2005, 4739.

41 C. Görller-Walrand and K. Binnemans, in *Handbook on the Physics and Chemistry of Rare Earths*, ed. K. A. Gschneidner Jr. and L. Eyring, Elsevier, Amsterdam, 1998, vol. 25, ch. 167.

42 R. Van Deun, D. Moors, B. De Fre and K. Binnemans, *J. Mater. Chem.*, 2003, **13**, 1520.

43 K. Driesen and K. Binnemans, *Liq. Cryst.*, 2004, **31**, 601.

44 L. J. Yu and M. M. Labes, *Appl. Phys. Lett.*, 1977, **31**, 719.

45 K. Binnemans and D. Moors, *J. Mater. Chem.*, 2002, **12**, 3374.

46 K. Binnemans, *Chem. Rev.*, 2005, **105**, 4148.

47 E. Guillet, D. Imbert, R. Scopelliti and J.-C. G. Bünzli, *Chem. Mater.*, 2004, **16**, 4063.

48 (*a*) M. Cantuel, G. Bernardinelli, G. Muller, J. P. Riehl and C. Piguet, *Inorg. Chem.*, 2004, **43**, 1840; (*b*) P. Gawryszewska, J. Legendziewicz, Z. Ciunik, N. Esfandiari, G. Muller, C. Piguet, M. Cantuel and J. P. Riehl, *Chirality*, 2006, **18**, 406.

 This journal is © The Royal Society of Chemistry 2006